

行政院國家科學委員會專題研究計畫 成果報告

雷射技術及時析光譜研究奈米光電材料與結構之研究(第3年)

研究成果報告(完整版)

計畫類別：個別型
計畫編號：NSC 96-2628-E-009-018-MY3
執行期間：98年08月01日至99年07月31日
執行單位：國立交通大學光電工程學系(所)

計畫主持人：謝文峰

計畫參與人員：博士班研究生-兼任助理人員：許智章
博士班研究生-兼任助理人員：歐伯濟
博士班研究生-兼任助理人員：陳厚仁
博士後研究：黃至賢

處理方式：本計畫可公開查詢

中華民國 99 年 08 月 23 日

行政院國家科學委員會補助專題研究計畫

成果報告

期中進度報告

雷射技術及時析光譜研究奈米光電材料與結構之研究

計畫類別： 個別型計畫 整合型計畫

計畫編號：NSC 96-2628-E-009 -018 -MY3

執行期間：96年08月01日至 99年07月31日

計畫主持人：謝文峰

共同主持人：

計畫參與人員：黃至賢、許智章、歐伯濟、陳厚仁。

成果報告類型(依經費核定清單規定繳交)： 精簡報告 完整報告

本成果報告包括以下應繳交之附件：

赴國外出差或研習心得報告一份

赴大陸地區出差或研習心得報告一份

出席新加坡與日本國際學術會議心得報告及發表之論文各一份

國際合作研究計畫國外研究報告書一份

處理方式：除產學合作研究計畫、提升產業技術及人才培育研究計畫、
列管計畫及下列情形者外，得立即公開查詢

涉及專利或其他智慧財產權， 一年 二年後可公開查

詢

執行單位：國立交通大學光電工程研究所

中 華 民 國 99年 8月 9 日

行政院國家科學委員會專題研究計畫成果報告
雷射技術及時析光譜研究奈米光電材料與結構之研究
計畫編號：NSC 96-2628-E-009 -018 -MY3
執行期限：97年8月1日至98年7月31日
主持人：謝文峰教授 國立交通大學光電工程系

一、中文摘要

藉著在室溫下測量薄ZnO磊晶薄膜的瞬時穿透差，我們觀察到超快自由激子的冷卻時間為700-900 fs之間；並獲得最大的誘發穿透發生在激子共振。另外，由激發強度相關的動態行為研究顯示激子鬆弛機制隨著激發強度增強會由激子-聲子散射轉變成激子-激子散射。

關鍵詞：非線性光學、半導體材料、非線性光學材料、超快量測、激子-聲子散射、和激子-激子散射。

Abstract

We observed ultrafast free exciton thermalization time of 700-900 fs and obtained the magnitude of maximal differential absorption to be $1.8 \times 10^4 \text{ cm}^{-1}$ with the pumping density of $10 \mu\text{J}/\text{cm}^2$ by measuring transient differential transmission in a thin ZnO epitaxial layer at room temperature. The largest induced transparency occurs near exciton resonance associated with absorption saturation by comparing the excitation from the above band-gap to band-tail states. The pump dependent dynamics reveals transition of the excitonic relaxation from the exciton-phonon scattering into the exciton-exciton scattering.

Keywords: Nonlinear optics, Semiconductor materials, Nonlinear optical materials, Ultrafast measurements.

二、緣由與目的

There has been great interest in optical properties of ZnO with the wide band-gap energy of 3.37 eV for the development of ultraviolet (UV) photonic devices.¹ Due to its large exciton binding energy of 60 meV as compared with other wide band-gap semiconductors,² such as ZnSe and GaN, free excitons exist in ZnO even at room temperature (RT). Besides, its large nonlinear absorption has been investigated by the Z-scan method near two-photon exciton resonance in near IR and near exciton resonance in UV range.^{3,4} RT optical pumped UV spontaneous emission (SPE), stimulated emission and lasing have been reported in ZnO thin films grown on sapphire substrates.^{5,6} The SPE is attributed to both the free exciton and near-band-edge emissions, whereas, the stimulated emission and lasing are related to exciton-exciton scattering and electron-hole-plasma (EHP) depending on the optical pumping intensity.

Transient absorption measurements have been commonly performed in GaN and related III-V materials on time scales of femtosecond (fs) to nanosecond (ns).⁷⁻⁹ For example, from the non-degenerate nanosecond pump-probe technique, GaN thin films reveal large optical nonlinearities associated with exciton saturation under high inter-band excitation.⁷ There are few studies on carrier dynamics in ZnO thin films and nanostructures by using transient absorption^{10,11} and time-resolved PL¹²⁻¹⁶ (TRPL) spectroscopy. Yamamoto et al. measured the carrier dynamics in ZnO thin films,¹⁰ and observed the saturation of exciton absorption as well as the optical gain on the lower energy side of free exciton by using the non-degenerate pump-probe method with high band-to-band excitation density of $90 \mu\text{J}/\text{cm}^2$. On the other hand, by using the optical Kerr gate (OKG) method to study the TRPL in ZnO thin films with exciton resonance pumping density of $70 \mu\text{J}/\text{cm}^2$, Takeda et al. reported that the formation of EHP takes less than 1 ps to build up.¹²

For the best performance of ZnO-based UV photonic devices, such as high-speed photonic devices and optical switches, quantitatively investigating the dynamical behavior and optical nonlinear absorption near free exciton resonance is necessary. In this work, besides the dynamics of the above band-gap states, the femtosecond degenerate pump-probe technique under resonant excitation was used to investigate free exciton thermalization by measuring the time-resolved differential transmission in a thin ZnO epitaxial layer at RT. An ultrafast relaxation time of 700-900 fs and maximal absorption saturation can be observed at exciton resonance. The investigation of pumping dependent dynamics suggests transition of excitonic relaxation from exciton-phonon scattering into exciton-exciton scattering under increase in pump density.

三、研究方法與步驟

Our c-axis oriented ZnO thin film with thickness of 70-nm was grown on a c-plane sapphire substrate by high-vacuum pulsed laser deposition (PLD) with KrF excimer laser. The detail growth apparatus and condition can be found in Ref. 17. The absorption spectrum was measured at RT (~295 K) by using the spectral photometer (Jasco V-670) with resolution of 0.5 nm. The time integrated PL excited by a frequency doubled

mode-locked Ti:sapphire laser with central wavelength of 360 nm was recorded by a single grating mono-chromator (iHR320) at RT. Similar to the system setup in previous studies,^{8,11,18} the measurement of transient absorption was carried out using the frequency doubled mode-locked Ti:sapphire laser with 82 MHz repetition rate (Tsunami, Spectral Physics Inc.), equipped with a frequency doubler (Model 3980), as the light source to provide UV excitation with wavelength ranging from 360 nm (3.444 eV) to 383 nm (3.238 eV). The laser output was divided by a beam-splitter into the pump and the probe beams. The pump beam was chopped at 1 KHz by a chopper. The pump and probe beams made a small angle of 8 degrees were focused on the sample by a 5 cm focal length lens with an intensity-contrast ratio of pump to probe larger than 20:1. The transmitted probe signal was detected by a photo-diode connected to a lock-in amplifier. A time delay between the pump and the probe beams was introduced by an optical delay line with a stepping motor. In order to reduce the coherent artifact, we kept the pump and the probe polarizations orthogonal to each other by using a half-wave plate and put a linear polarizer with the polarization parallel to the probe beam before the detector.

四、結果與討論

Figure 1 shows the absorption and time-integrated photoluminescence (TIPL) spectrum of the 70-nm ZnO epitaxial layer grown on c-plane sapphire at room temperature (RT). It reveals an absorption peak near 373 nm (3.324 eV) corresponding to the free exciton transition and another peak at 366.4 nm (3.384 eV) to the band-gap. The energy difference of absorption peaks of 60 meV corresponds to the free exciton binding energy of bulk ZnO and the linear absorption coefficient of free exciton transition is estimated to be around $2.2 \times 10^5 \text{ cm}^{-1}$, also comparable to the value measured in ZnO single crystals.¹⁹ The TIPL spectrum at RT under 1 and 10 $\mu\text{J}/\text{cm}^2$ excitation reveals the emission peak around 376 nm (3.298 eV) corresponding to free exciton transition with FWHM of 102 meV. It is comparable to previous result reported by Yamamoto et al.,¹⁰ in which the peak position of observed PL spectra is located at 3.299 eV due to free exciton radiative recombination at RT. It is also consistent with the result in Fig. 3 of Ref. 21, in which the PL peak is 3.43 eV (??) at 10K and ~ 3.3 eV at RT. Due to large exciton-LO-phonon coupling in ZnO,^{20,21} several peaks on the lower energy shoulder are the exciton related LO-phonon replica. The observed RT TIPL spectra show no apparent shift even with pumping density up to 30 $\mu\text{J}/\text{cm}^2$. In addition, the presence of the exciton related LO-phonon replica in Fig. 1 indicates no emergence of EHP because the screening of Coulomb interaction by EHP should diminish the exciton and LO-phonon coupling. Thus, the observed TIPL spectra should be attributed to free exciton spontaneous emission at RT; it is not the red-shifted EHP emission resulting from the band gap renormalization (BGR) observed at low temperature.

The free carrier dynamics pumped by photon wavelength at 365 nm (3.397 eV) at $\sim 10 \mu\text{J}/\text{cm}^2$ excitation, corresponding to near band-gap excitation, is shown in Fig. 2. At the beginning of the pulse excitation, an instantaneous rise around zero time delay can be seen, and then the photo-generated free carriers quickly occupy the above band-gap states to quench the further absorption that is what the band-filling is observed. The trace after zero time delay can be found consisting of a fast and a slow decay. Generally speaking, the photo-excited free carriers are scattered out of their initial states through carrier-carrier interaction, which is comparable to the time scale around pulse duration, and then quickly relax to reach the quasi-equilibrium with the lattice system through carrier-phonon interaction. Thus, the decrease of transient differential transmission can be attributed to the free carriers consume their kinetic energy via carrier-carrier and carrier-phonon scattering to the band-edge or to form excitons.

The normalized transient differential transmissions ($\Delta T/T$) near free exciton transition as a function of time delay for excitation wavelengths at 372 nm (3.333 eV) and 373 nm (3.324 eV) also with $\sim 10 \mu\text{J}/\text{cm}^2$ excitation are shown in Fig. 3. Their temporal behavior is similar to that performed at near band-gap (3.397 eV) excitation. Because the excitonic states are simply occupied by the resonantly generated excitons, the absorption saturation by the band-filling (BF) can be achieved.²⁴ The absorption saturation due to the occupancy of non-equilibrium excitons is sufficient to produce decrease of absorption resulting in a measurable differential transmission even with spatially averaging over the probe beam profile, which is just slightly smaller than the pump one. The fast recovery of absorption saturation can be attributed to excitonic thermalization process through phonon emission. After the thermalization, the decrease in exciton population via either radiative or non-radiative recombination causes the slow recovery.

In order to extract the time constants of free carrier relaxation, the response function of $A_1 \exp(-t/\tau_1) + A_2 \exp(-t/\tau_2)$ was used to fit the trace in Fig. 2. Here, the coefficient A_1 and A_2 is corresponding to the fast and slow exponential decay component contributed to the BF effect, respectively. The fast decay time τ_1 of 0.77 ps is consistent with the hot carrier cooling time on the order of 1 ps reported by Yamamoto et al. in ZnO thin films.¹⁰ Besides, the obtained slow decay time τ_2 of 7.65 ps is close to the non-radiative recombination time on the order of 10 ps in ZnO nanorods.¹¹ On the other hand, the best fitting for the

excitation at 372 and 373 nm in Fig. 3 were achieved in use of three decay times as: $A_1\exp(-t/\tau_1)+A_2\exp(-t/\tau_2)+A_3\exp(-t/\tau_3)$. An ultrafast time constant τ_1 of 0.82-0.85 ps can be obtained due to excitonic thermalization. According to previous TRPL studies of EHP dynamics in ZnO thin films by using the optical Kerr gate method,¹² the red shift of PL emission was observed with a time constant less than 1 ps during the build-up stage of EHP state. Because the formation of EHP state is concerned about photo-excited enough carriers to achieve the Mott transition, the screening of Coulomb interaction and the band-gap renormalization effects need to be considered during the relaxation process. However, we pumped the sample here with lower excitation density and monitored the intrinsic non-equilibrium excitonic state. Thus, the reported ultrafast relaxation time of 0.82-0.85 ps is mainly due to the thermalization process through exciton-phonon or exciton-exciton scattering. Furthermore, the time constant τ_2 of 8.46-8.95 ps should be predominately caused by the non-radiative channels, such as trapping by defects, multi-phonon emission, or Auger recombination. And the time constant τ_3 of 47.8-53.2 ps is attributed to the longer radiative lifetime, which is comparable to the previous TRPL studies that the spontaneous recombination time is on the order of 46 to 110 ps in ZnO films grown by MBE and 30 to 74 ps in rf-sputtered films.^{15,16}

The maximal normalized differential transmission as a function of excitation energy from the above band-gap to the band-tail states was plotted in Fig. 4. The largest induced transparency due to absorption saturation occurs at 372.5 nm (3.329 eV), corresponding to the free exciton transition, is consistent with the absorption spectrum in Fig. 1. It can be obviously observed that the maximum of $\Delta T/T$ near the free exciton transition (372.5 nm) is five-times larger than the value near the band-gap state (365 nm) in Fig. 4, although their linear absorption coefficient is almost the same. It is similar to the investigation of transient absorption in GaAs and ZnTe quantum wells at RT,^{24,25} that the bleached exciton absorption by excited resonant excitons is stronger than the same density of free electron-hole pairs. It implies that the absorption saturation of free exciton via resonant excitation is more efficient than that of band-edge absorption due to not only inter-band transition but also free-carrier absorption. Because the measured differential reflectivity ($\Delta R/R$) is on the order of 10^{-3} , whereas the measured differential transmission ($\Delta T/T$) is on the order of 10^{-1} , we neglected the change of reflectance and deduced the differential absorption from the differential transmission based on the equation of: $\Delta\alpha = -\frac{1}{d}\ln(1 + \frac{\Delta T}{T})$ with d being the thickness of sample. The value of $\Delta\alpha$ is estimated to be $-1.8 \times 10^4 \text{ cm}^{-1}$ near exciton resonance under $10 \mu\text{J}/\text{cm}^2$ pumping that is comparable to the results measured in GaN at 10K and in GaAs at 15K measured with the differential transmission spectrum (DTS) by using the pump-probe technique.^{7,26}

In order to realize the mechanism of free exciton thermalization, we performed the pumping dependent dynamics and nonlinear absorption near exciton resonance. Figure 5 shows the free exciton dynamics for three different pumping densities. We found the ultrafast relaxation time on the order of 800-900 fs is almost independent of the pumping density under $1\text{-}20 \mu\text{J}/\text{cm}^2$. This ultrafast relaxation time is responsible for free exciton thermalization via exciton and phonon scattering. However, the relaxation time slightly decreases to 700-800 fs as increasing the pumping density to $30\text{-}50 \mu\text{J}/\text{cm}^2$. By using the optical Kerr gate measurements, previous TRPL studies reported the build-up of P-band emission with a time constant of 800 fs through exciton-exciton scattering in ZnO thin films.¹³ Consequently, the decrease of relaxation time with increasing pumping density supports the transition of excitonic thermalization from exciton-phonon scattering at low pumping into exciton-exciton scattering at high pumping.

The negative differential absorption maximum as a function of pumping density is shown in Fig. 6. The temporal regime of the measured differential absorption on the order of pulse duration is shorter than the relaxation process. We can mainly attribute the negative differential absorption to the band-filling of resonantly excited excitons, while the screening effect from the free carriers via exciton-LO-phonon interaction may play a minor role.^{24,25} To estimate the saturation intensity, we fit the experimental results by using the absorption saturation model,²⁷

$$\left| \frac{\Delta\alpha}{\alpha_0} \right| = \frac{(1-x)(I/I_s)}{1+I/I_s}, \quad (1)$$

where $\Delta\alpha$ is the differential absorption maximum within the pulse duration, α_0 is the absorption coefficient without pumping, x is the non-saturated portion of absorption and I_s is the saturation intensity. We obtained $x = 0.65$ and $I_s = 25 \mu\text{J}/\text{cm}^2$. It means that about 35% of resonantly excited excitons contribute to the band-filling. The value of negative differential absorption maximum shows a linear dependence of

pumping density ranging from 1 to 20 $\mu\text{J}/\text{cm}^2$. With higher excitation, the value reveals a nonlinear dependence of pumping density. Therefore, the screen effect due to the BGR may emerge to diminish the effect of band filling between 20 and 25 $\mu\text{J}/\text{cm}^2$. We estimated the carrier density at the emergence of nonlinearity about $7 \times 10^{18} \text{ cm}^{-3}$. As pumping density larger than 50 $\mu\text{J}/\text{cm}^2$, a constant value of $\Delta\alpha \sim 4.7 \times 10^4 \text{ cm}^{-1}$ will be reached. Similar results were reported in GaN thin films at 4 K under exciton resonant excitation.⁹

五、結論

In conclusion, the energy dependent dynamics in a thin ZnO epitaxial layer have been investigated by using the femtosecond pump-probe technique at room temperature. Transient absorption measurement shows an ultrafast relaxation time of 800-900 ps due to free exciton thermalization, and the differential absorption ($\Delta\alpha \sim -1.8 \times 10^4 \text{ cm}^{-1}$) under the pumping density of 10 $\mu\text{J}/\text{cm}^2$. When the excited excitonic density increases, the relaxation time decreases to 700 fs and the magnitude of $\Delta\alpha$ gradually approaches a constant value. In addition, the largest induced transparency associated with absorption saturation occurs near exciton resonance. The pumping dependent dynamics reveals transition of free exciton thermalization process from exciton-phonon scattering into exciton-exciton scattering.

六、自我評估

本三年期計畫中我們進行雷射技術及時析光譜研究奈米光電材料與結構之研究共發表8篇SCI論文。另外，在光電物理之研究方面分別研究氧化(鎂)鋅薄膜與量子點之成長與光電性質和光子晶體波導之理論。我們利用雷射濺鍍與sol-gel法成功地成長氧化(鎂)鋅薄膜與量子點等。成長之樣品我們分別研究，激子—聲子之交互作用、螢光、受激輻射與雷射現象、拉曼散射等等。在光子晶體波導研究方面，我們以緊束縛原理首次成功地解釋光子晶體波導的偶合與不偶合現象。三年來共發表31篇光電物理相關的SCI論文，成果還算不錯。

七、參考文獻

- ¹ T. Makino, C. H. Chia, N. T. Tuan, Y. Segawa, M. Kawasaki, A. Ohtomo, K. Tamura, and H. Koinuma, *Appl. Phys. Lett.* **76**, 3549 (2000).
- ² Y. F. Chen, D. M. Bagnall, H. J. Koh, K. T. Park, K. Hiraga, Z. Q. Zhu, and T. Yao, *J. Appl. Phys.* **84**, 3912 (1998).
- ³ J. H. Lin, Y. J. Chen, H. Y. Lin, and W. F. Hsieh, *J. Appl. Phys.* **97**, 033526 (2005).
- ⁴ Y. P. Chan, J. H. Lin, C. C. Hsu, and W. F. Hsieh, *Optics Express* **16**, 19900 (2008).
- ⁵ D. M. Bagnall, Y. F. Chen, Z. Q. Zhu, T. Yao, S. Koyama, M. Y. Shen, and T. Goto, *Appl. Phys. Lett.* **70**, 2230 (1997).
- ⁶ P. Zu, Z. K. Tang, G. K. L. Wong, M. Kawasaki, A. Ohtomo, H. Koinuma, and Y. Segawa, *Solid State Commun.* **103**, 459 (1997).
- ⁷ T. J. Schmidt, J. J. Song, Y. C. Chang, R. Horning, and B. Goldenberg, *Appl. Phys. Lett.* **72**, 1504 (1998).
- ⁸ C. K. Sun, J. C. Liang, X. Y. Yu, S. Keller, U. K. Mishra, and S. P. DenBaars, *Appl. Phys. Lett.* **78**, 2724 (2001).
- ⁹ S. Hess, R. A. Taylor, K. Kyhm, J. F. Ryan, B. Beaumont, and P. Gibart, *Phys. Stat. Sol. (b)* **216**, 57 (1999).
- ¹⁰ A. Yamamoto, T. Kido, T. Goto, Y. F. Chen, T. Yao, and A. Kasuya, *Appl. Phys. Lett.* **75**, 469 (1999).
- ¹¹ C. K. Sun, S. Z. Sun, K. H. Lin, K. Y. J. Zhang, H. L. Liu, S. C. Liu and J. J. Wu, *Appl. Phys. Lett.* **87**, 023106 (2005).
- ¹² J. Takeda, H. Jinnouchi, S. Kurita, Y. F. Chen, and T. Yao, *Phys. Stat. Sol. (b)* **229**, 877 (2002).
- ¹³ Y. Toshihira, J. Takeda, H. J. Ko, and T. Yao, *Phys. Stat. Sol. (c)* **1**, 839 (2004).
- ¹⁴ J. Fallert, F. Stelzl, H. Zhou, A. Reiser, K. Thonke, R. Sauer, C. Klingshirn, and H. Kalt, *Optics Express* **16**, 1125 (2008).
- ¹⁵ T. Koida, A. Uedono, A. Tsukazaki, T. Soto, M. Kawasaki, and S. F. Chichibu, *Phys. Stat. Sol. (a)* **201**, 2841 (2004).
- ¹⁶ Ü. Özgür, A. Teke, C. Liu, S. J. Cho, H. Morkoc, and H. O. Everitt, *Appl. Phys. Lett.* **84**, 3223 (2004).
- ¹⁷ W. R. Liu, W. F. Hsieh, C. H. Hsu, K. S. Liang, and F. S. S. Chien, *J. Crystal Growth* **297**, 294 (2006).
- ¹⁸ A. Von Lehmen, J. E. Zucker, J. P. Heritage, D. S. Chemla, and A. C. Gossard, *Appl. Phys. Lett.* **48**, 1479 (1986).
- ¹⁹ W. Y. Liang and A. D. Yoffe, *Phys. Rev. Lett.* **20**, 59 (1968).
- ²⁰ C. Klingshirn, *Phys. Stat. Sol. (b)* **244**, 3027 (2007).
- ²¹ C. Klingshirn, R. Hauschild, J. Fallert, and H. Kalt, *Phys. Rev. B* **75**, 115203 (2007).
- ²² Y. F. Chen, N. T. Tuan, Y. Segawa, H. J. Ko, S. K. Hong, and T. Yao, *Appl. Phys. Lett.* **78**, 1469 (2001).
- ²³ E. Hendry, M. Koeberg, and M. Bonn, *Phys. Rev. B* **76**, 045214 (2007).
- ²⁴ W. H. Knox, R. L. Fork, M. C. Downer, D. A. B. Miller, D. S. Chemla, C. V. Shank, A. C. Gossard, and W. Wiegmann, *Phys. Rev. Lett.* **54**, 1306 (1985).
- ²⁵ P. C. Becker, D. Lee, A. M. Johnson, A. G. Prosser, R. D. Feldman, R. F. Austin, and R. E. Behringer, *Phys. Rev. Lett.* **68**, 1876 (1992).
- ²⁶ S. W. Koch, N. Peyghambarian, and M. Lindberg, *J. Phys. C* **21**, 5229 (1988).
- ²⁷ Y. Wang, A. Suna, J. McHugh, E. F. Hilinski, P. A. Lucas, and R. D. Johnson, *J. Chem. Phys.* **92**, 6927 (1990).

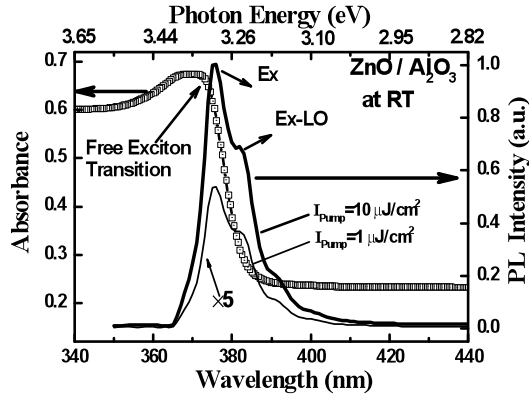


FIG. 1. Absorption spectrum (hollow squares) and TIPL spectra (solid lines) with excitation of $1 \mu\text{J}/\text{cm}^2$ (thin line) and $10 \mu\text{J}/\text{cm}^2$ (thick line) from a thin ZnO epitaxial layer at RT.

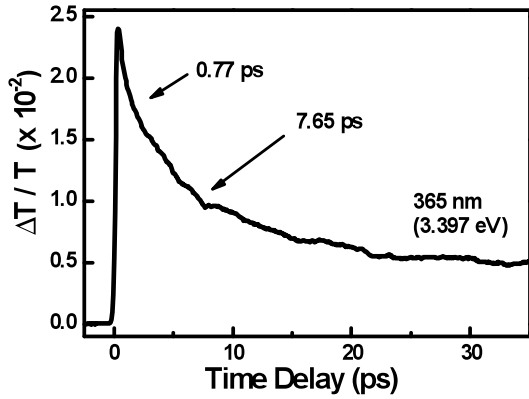


FIG. 2. Measured normalized transient differential transmission as a function of time delay with photo-excited energy above band-gap states.

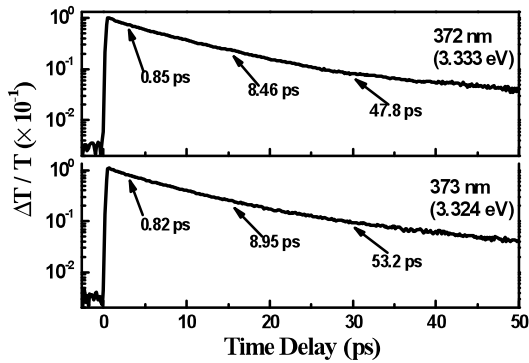


FIG. 3. Normalized transient differential transmission for photon wavelength at 372 and 373 nm.

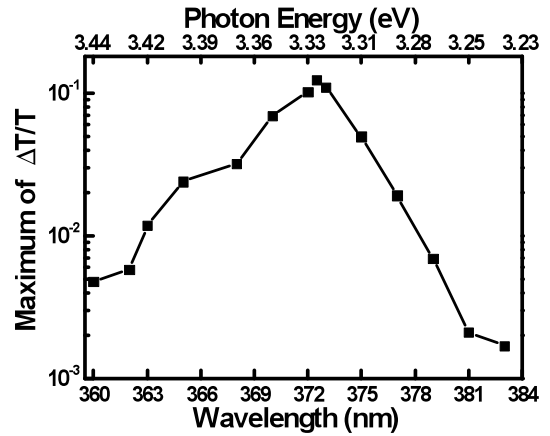


FIG. 4. The maximal differential transmission as a function of excitation wavelength under pumping density of $10 \mu\text{J}/\text{cm}^2$.

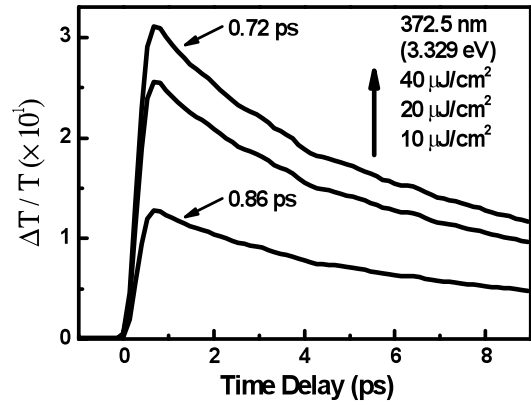


FIG. 5. Measured normalized transient differential transmission as a function of time delay for photon wavelength at 372.5 nm under pumping density of (from bottom to top) 10, 20 and $40 \mu\text{J}/\text{cm}^2$.

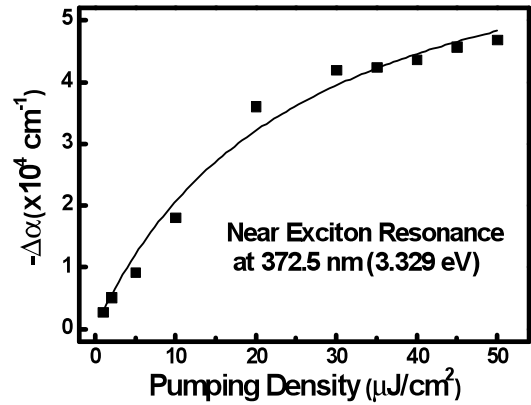


FIG. 6. A plot of negative differential absorption maximum as a function of pumping density (solid squares) with excitation near exciton resonance for wavelength at 372.5 nm. The solid curve represents the fitting curve to Eq. (1) and the dashed lines plotted to guide the eyes revealing a turning point at pumping density of $20 \mu\text{J}/\text{cm}^2$.

無研發成果推廣資料

96 年度專題研究計畫研究成果彙整表

計畫主持人：謝文峰		計畫編號：96-2628-E-009-018-MY3				計畫名稱：雷射技術及時析光譜研究奈米光電材料與結構之研究	
成果項目		量化			單位	備註（質化說明：如數個計畫共同成果、成果列為該期刊之封面故事...等）	
		實際已達成數（被接受或已發表）	預期總達成數（含實際已達成數）	本計畫實際貢獻百分比			
國內	論文著作	期刊論文	0	0	100%	篇	
		研究報告/技術報告	0	0	100%		
		研討會論文	1	1	100%		
		專書	0	0	100%		
	專利	申請中件數	0	0	100%	件	
		已獲得件數	0	0	100%		
	技術移轉	件數	0	0	100%	件	
		權利金	0	0	100%	千元	
	參與計畫人力 （本國籍）	碩士生	0	0	100%	人次	
		博士生	2	0	100%		
博士後研究員		1	0	100%			
專任助理		0	0	100%			
國外	論文著作	期刊論文	8	3	100%	篇	
		研究報告/技術報告	0	0	100%		
		研討會論文	1	1	100%		
		專書	0	0	100%	章/本	
	專利	申請中件數	0	0	100%	件	
		已獲得件數	0	0	100%		
	技術移轉	件數	0	0	100%	件	
		權利金	0	0	100%	千元	
	參與計畫人力 （外國籍）	碩士生	0	0	100%	人次	
		博士生	0	0	100%		
博士後研究員		0	0	100%			
專任助理		0	0	100%			

<p>其他成果 (無法以量化表達之成果如辦理學術活動、獲得獎項、重要國際合作、研究成果國際影響力及其他協助產業技術發展之具體效益事項等，請以文字敘述填列。)</p>	無。
--	----

	成果項目	量化	名稱或內容性質簡述
科 教 處 計 畫 加 填 項 目	測驗工具(含質性與量性)	0	
	課程/模組	0	
	電腦及網路系統或工具	0	
	教材	0	
	舉辦之活動/競賽	0	
	研討會/工作坊	0	
	電子報、網站	0	
	計畫成果推廣之參與(閱聽)人數	0	

國科會補助專題研究計畫成果報告自評表

請就研究內容與原計畫相符程度、達成預期目標情況、研究成果之學術或應用價值（簡要敘述成果所代表之意義、價值、影響或進一步發展之可能性）、是否適合在學術期刊發表或申請專利、主要發現或其他有關價值等，作一綜合評估。

1. 請就研究內容與原計畫相符程度、達成預期目標情況作一綜合評估

達成目標

未達成目標（請說明，以 100 字為限）

實驗失敗

因故實驗中斷

其他原因

說明：

2. 研究成果在學術期刊發表或申請專利等情形：

論文： 已發表 未發表之文稿 撰寫中 無

專利： 已獲得 申請中 無

技轉： 已技轉 洽談中 無

其他：（以 100 字為限）

本三年計畫我們進行雷射技術及時析光譜研究奈米光電材料與結構之研究共發表 14 篇 SCI 論文。另外，在光電物理之研究方面三年來共發表 25 篇光電物理相關的 SCI 論文，成果還算不錯。

3. 請依學術成就、技術創新、社會影響等方面，評估研究成果之學術或應用價值（簡要敘述成果所代表之意義、價值、影響或進一步發展之可能性）（以 500 字為限）

光電半導體材料之非線性光學與載子動態行為之研究成果包括：(i) 利用 Z-scan 法量測 ZnO 薄膜，發現接近 ZnO 激子共振雙光子與單光子共振增強非線性吸收。(ii) 利用瞬時穿透量測觀察埋在 300nm 厚內之 6 nm 寬 InGaAsN 單量子井之超快載子動態行為，其結果與時析螢光光譜所觀察之現象相符。最近應用於 50nm 超薄 ZnO 薄膜之超快載子動態行為，發現 band filling 效應和 band gap renormalization 效應相互競爭，此現象在較厚之樣品，如 1mm 樣品中不易被觀察。在雷射動力學三項成果：(i) 首次在簡併共振腔附發現雷射輸出光為瓶形光束；這種瓶形光束可被用於捕捉原子之用。(ii) 光子晶體光纖產生 350-1600nm 之寬頻超連續光。(iii) 固態雷射中加入非線性鏡或飽合吸收晶體(或飽合吸收反射鏡)，得到 Q-開關鎖模或連續鎖模之脈衝雷射輸出。光子晶體中傳輸與量子光電研究等。

